Comparison of LNA Topologies for WiMAX Applications in a Standard 90-nm CMOS Process

Michael Angelo G. Lorenzo
Electrical and Electronics Engineering Institute
University of the Philippines, Diliman
Quezon City, Philippines
mglorenzo1@up.edu.ph

Maria Theresa G. de Leon
Electrical and Electronics Engineering Institute
University of the Philippines, Diliman
Quezon City, Philippines
tess@eee.upd.edu.ph

***Abstract*— This paper presents the design of low-noise amplifiers intended for WiMAX applications. Three low-noise amplifier topologies are implemented namely: (1) cascoded common-source amplifier, (2) folded cascode amplifier, and (3) shunt feedback amplifier. The amplifiers were implemented in a standard 90-nm CMOS process and were operated with a 1-V supply voltage. Low-noise amplifier measurements were taken for parameters such as power gain, noise figure, input matching, output matching, reverse isolation, stability, and linearity. Based on the employed figure-of-merit, the cascoded common-source low-noise amplifier achieved the best performance among the three with a simulated gain of 13.8 dB and noise figure of 1.7 dB, which makes it comparable to previously published works.**

Keywords- RF IC Design; Low-noise amplifier; WiMAX; Wireless communications

I. INTRODUCTION

The rapid acceleration of advances in CMOS scaling and RF CMOS circuit design techniques in the past few years have made it possible to integrate all the elements of a transceiver on a single chip. Inexpensive CMOS technologies have been used successfully to implement all the necessary RF functionality for existing and emerging wireless area network standards, such as Bluetooth and WiMAX [1]. In 2005, a CMOS system-on-chip (SOC) solution to enable a single-chip phone, where the analog and digital basebands, power management, and the RF transceiver are fully integrated on a single monolithic CMOS IC, has been reported [2].

WiMAX is a telecommunications technology which stands for Worldwide Interoperability for Microwave Access. It belongs to the IEEE 802.16 family of standards, which aim to provide wireless broadband access. It provides data rates of up to 100 Mbps at 20 MHz bandwidth [3]. It has a very large coverage area of around 50 km. for one base station which makes it a viable option for implementation of last-mile connectivity. There are two types of WiMAX systems: Fixed WiMAX and Mobile WiMAX. The fixed WiMAX system does not allow handoff between base stations. Mobile WiMAX on the other hand provides both mobile and fixed services [4].

The rest of the paper proceeds as follows: Section 2 of this paper presents the topologies of the implemented low-noise amplifiers. The discussion of the circuit design follows in section 3. The simulation results are presented in section 4 followed by the conclusion in section 5.

II. LOW-NOISE AMPLIFIERS

The low-noise amplifier (LNA) is the first block in the receiver chain of a communications system, connected directly to the antenna. Its noise figure (NF) performance has the most impact to the overall receiver system. Its task is to amplify the very weak signals coming from the antenna while adding as little noise as possible. NF is a crucial design specification which trades off with other design parameters such as third order input intercept point (IIP3), second order input intercept point (IIP2), gain, and power consumption.

A. Cascoded Common Source Amplifier

The most commonly used topology for LNA design today is the cascode amplifier with inductive source degeneration shown in the Fig. 1. This type of cascode amplifier is called the telescopic cascode amplifier since the cascode transistor is the same type as the input transistor. On the other hand, a folded cascode amplifier has a cascode transistor with a different type from the input transistor [5].

The cascode topology results in a higher gain, due to the increase in the output impedance, as well as better isolation between the input and output ports. The cascode transistor M2 suppresses the Miller capacitance of M1 thereby increasing the reverse isolation [6]. The suppression of the parasitic capacitances of the input transistor also improves the high frequency operation of the amplifier.

B. Folded Cascode Amplifier

A topology that is suitable if the LNA is intended for very low-voltage application is the folded cascode topology shown in Fig. 2. Since the NMOS and PMOS transistor are placed in parallel between the supply and ground rail, it is able to operate for lower supply voltages compared to the telescopic cascode amplifiers. The PMOS cascode transistor M2 reduces the input capacitance and provides good reverse isolation and enhances stability [7].

978-0-7695-4016-0/10 $26.00 © 2010 IEEE
DOI 10.1109/UKSIM.2010.122

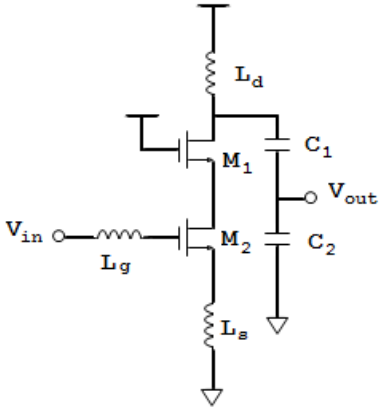

Figure 1 Cascoded common-source amplifier.

C. *Shunt Feedback Amplifier*

The shunt-feedback LNA is shown in Fig. 3. It supports simultaneous input and output match over a large frequency range and it is able to achieve a very high linearity. The linearity of the amplifier improves since the gain, which is largely set by feedback, becomes less sensitive to the gain of the amplifier. The feedback elements, which are composed of a resistor in series with a capacitor, linearize the gain and increase the bandwidth of the amplifier. Using feedback is also suited for the CMOS LNA since the input impedance of MOSFETs is large and mostly capacitive, which means that the input impedance can be controlled and set by feedback. To improve the high-frequency performance, an additional inductor can be placed in series with the resistor and capacitor [8].

III. CIRCUIT DESIGN

The performance requirement for a WiMAX receiver is listed in Table 1. These receiver specifications are obtained from the IEEE 802.16 standard released in 2004 [9]. The next part of the design involves the mapping of the specifications from the IEEE standard to relevant system-level parameters such as Bit Error Ratio (BER), Signal-to-Noise Ratio (SNR), and receiver sensitivity. These system-level specifications are then mapped into block-level using link budget analysis [10].

Table 2 summarizes the block-level specifications for the LNA. The LNA must be able to achieve high gain and low noise figure to relax the gain requirement of the mixer and at the same time give the whole receiver a low noise figure. The noise figure also determines the minimum input signal that can be resolved by the LNA while the linearity dictates the maximum input signal level that will not cause nonlinear operation. The LNA, having a finite reverse isolation and being connected directly to the antenna, needs a good input and output match to prevent signals from leaking back to the antenna and getting re-transmitted causing unwanted interference.

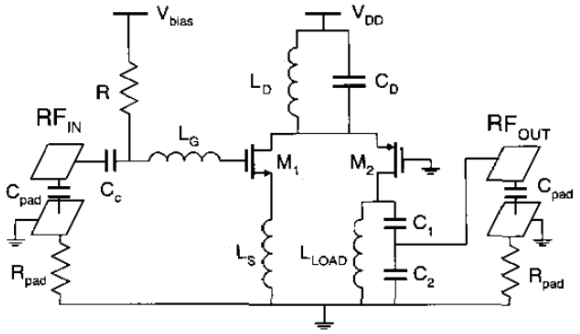

Figure 2 Folded cascode amplifier.

A. *Cascoded Common Source Amplifier*

The formula for the input impedance of the cascoded common-source LNA is given in (1) where gm, Cgs, Lg, and Ls are the input transistor's transconductance, input transistor's gate-to-source capacitance, gate inductance, and source inductance respectively..At the resonant frequency, given in (2), the formula for the input impedance reduces to (3). The width of the input transistor M1 that will give the required transconductance was set based on (2). The degenerating inductor Ls, which gives the LNA its purely real input impedance, was computed based on (3). With the value of Ls determined, the value of the gate inductance, Lg, that will set the resonant frequency, can be calculated. The width of the cascode transistor M2, was set equal to the width of the input transistor to take advantage of the reduced junction capacitance in the layout. Finally, the output matching network, composed of the drain inductor, Ld, and the output capacitors, C_1 and C_2, can be designed. Fig. 4 shows the final schematic design of the cascoded common-source with device sizes and bias voltages.

$$Z_{in} = \left(\frac{g_m}{C_{gs}}\right) * L_s + \frac{1}{s * C_{gs}} + s(L_g + L_s). \quad (1)$$

$$\omega_o = \frac{1}{\sqrt{(L_g + L_s)C_{gs}}}. \quad (2)$$

$$Z_{in} = \left(\frac{g_m}{C_{gs}}\right) * L_s \quad \text{(At resonance)}. \quad (3)$$

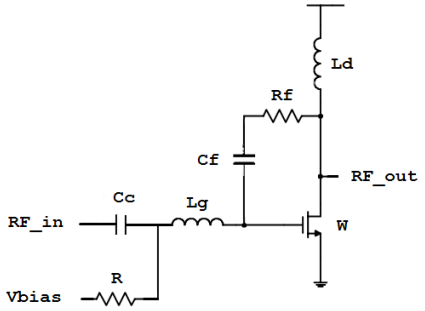

Figure 3 Shunt feedback amplifier.

TABLE I. WiMAX receiver performance requirements

Rx max. input level on-channel reception tolerance	≥ -30 dBm
Rx max. input level on-channel damage tolerance	≥ 0 dBm
1st adjacent channel rejection	≥ 4 dBm
2nd adjacent channel rejection	≥ 23 dBm
Image rejection	≥ 60 dBm
Channel Bandwidth	2 to 20 MHz
Noise Figure	≤ 7dB

TABLE II. Receiver front-end block-level specifications

Parameter	LNA
Gain	20 dB
Noise Figure	3 dB
Linearity	-10 dBm
Input and Output Matching	< -10dB

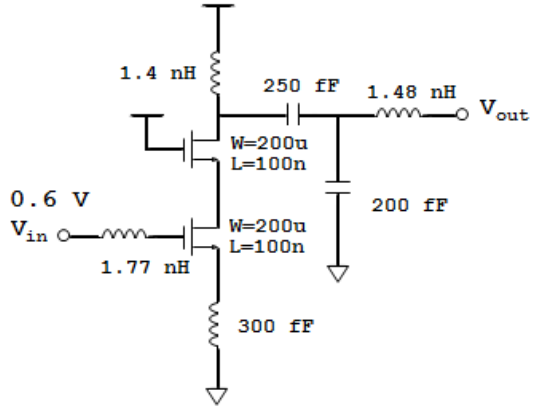

Figure 4 Schematic design of cascoded common-source amplifier.

B. *Folded Cascode Amplifier*

The design of the folded cascode LNA is very similar to the design of the telescopic cascode LNA. The source inductance Ls sets the real input impedance while the gate inductance Lg is computed based on the resonance frequency. The inductor Ld resonates with the drain junction capacitance of M1 and the source junction capacitance of M2. The inductor L_{LOAD} and capacitors C_1 and C_2, make up the output matching network. The final schematic design of the folded cascode LNA is shown in Fig. 5.

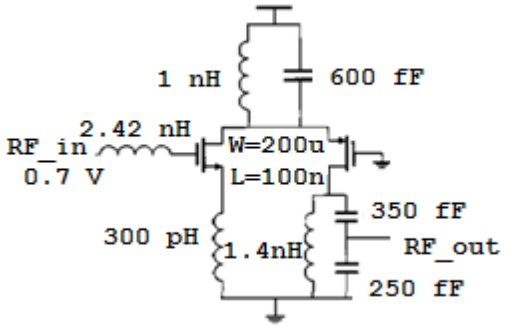

Figure 5 Schematic design of folded cascode amplifier.

C. *Shunt Feedback Amplifier*

For the design of the shunt feedback LNA, the value of the feedback resistor which sets the power gain is given in (4) where Rf, Zo, and S21 are the values of the feedback resistor, output impedance, and the transducer gain. A small inductor was placed in the gate of the transistor to aid in matching. A load inductor was placed in the drain of the transistor to tune out the junction capacitances in the drain of the transistor. The value of the feedback capacitor, which is used for biasing purposes, was set large enough to not have a significant effect on feedback. Finally, the shunt feedback amplifier was duplicated and connected in cascade with a coupling capacitor in between giving the cascaded shunt feedback amplifier a gain of 20 dB. The schematic design of the cascaded shunt amplifier is shown in Fig. 6

$$R_f = Z_o(1+|S_{21}|). \tag{4}$$

IV. Simulation Results

The LNA topologies were implemented in a standard 90-nm CMOS process. The extraction of all device parameters for use in simulations was done using *Synopys® StarRCXT*. Simulation of the extracted view was done using *Cadence® Design System Software*. The low-noise amplifiers were designed to operate at the Unlicensed National Information Infrastructure (U-NII) band of 5.725 GHz to 5.825 GHz. Measurements in the plots were taken at 5.8 GHz.

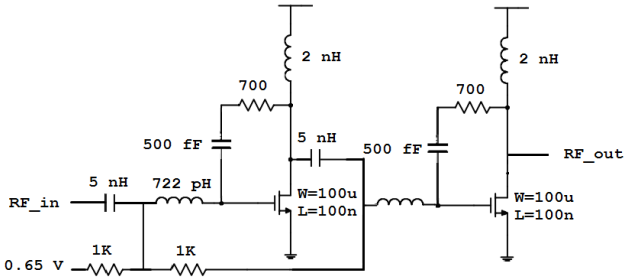

Figure 6 Schematic design of shunt feedback amplifier.

The plots of the simulation results are shown in the figures below. Fig. 7 shows the plot of the power gain. The shunt feedback amplifier achieved the highest gain with 19.792 dB followed by the cascoded common-source with 13.796 dB and the folded cascode achieved the lowest gain with a gain of 12.893 dB. As can be seen on the plot of the power gain, the shunt feedback amplifier has a relatively wideband characteristic compared to the cascode amplifiers. The linearizing effect of feedback gives the shunt feedback amplifier its wideband characteristic compared to the narrowband characteristic of the cascode amplifiers.

The plot of the total DSB noise figure is shown in Fig. 8. The extracted noise figures of the LNA topologies are as follows: 1.7 dB for the cascoded common-source, 1.79 dB for the folded cascode, and 2.63 dB for the shunt feedback amplifier. All the LNA topologies achieved a noise figure below 3 dB. As with the power gain plot, the shunt feedback amplifier achieved the most linear noise figure plot among the three. The plot of the stability factor is shown in Fig. 9. The three amplifiers are unconditionally stable with stability factor greater than 1 at the frequency of interest.

Table 3 summarizes the simulation results for input voltage reflection coefficient (S11), output voltage reflection coefficient (S22), and reverse isolation or reverse gain (S12).

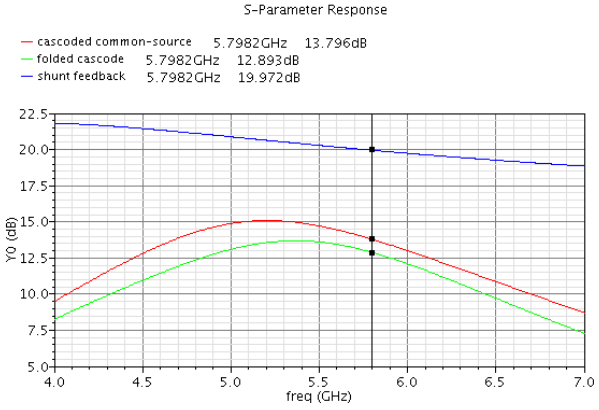

Figure 7 Power gain.

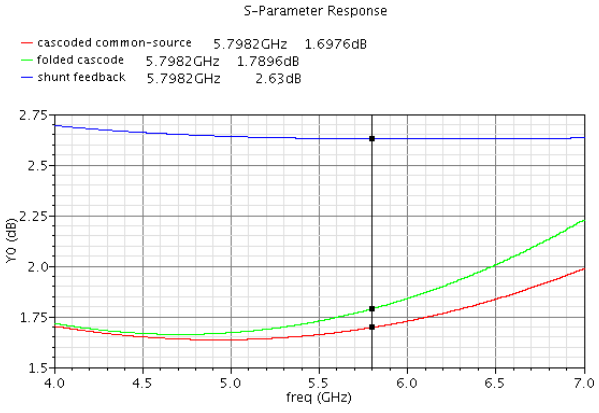

Figure 8 Noise figure.

TABLE III. Summary of s-paramaters

Topology	S11(dB)	S22(dB)	S12(dB)
Cascoded common-source	-9.45	-14.47	-23.6
Folded cascode	-12.33	-8.98	-25.99
Shunt feedback	-11.33	-22.8	-31.14
Target	-10	-10	-20

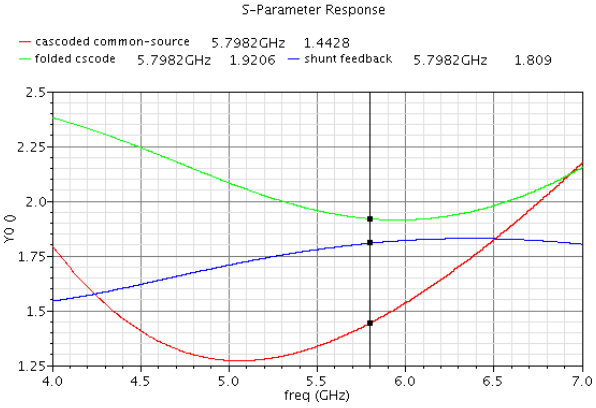

Figure 9 Stability coefficient.

Only the cascoded common-source, with S11 of -9.45 dB, was not able achieve the -10 dB target value for S11 while only the folded cascode, with S22 of -8.98 dB, was not able to achieve the -10 dB target value for S22. All the amplifiers achieved a reverse isolation better than -20 dB. The cascaded shunt feedback LNA being a two-stage amplifier achieved the best reverse isolation with 31.14 dB.

The amplifier's linearity was measured using the input-referred third-order intercept point (IIP3). Fig. 10-12 shows the linearity plots for the three amplifiers. All three amplifiers achieved the target IIP3 of -10 dBm. The improved linearity due to feedback gave the shunt feedback amplifier the best linearity among the three with an IIP3 of -5.03 dBm.

To compare the different LNA topologies, a figure-of-merit, derived in [11] is used. This figure-of-merit is a revised form of the gain-to-dc-power-consumption figure-of-merit which incorporates linearity in the form of the input-referred third-order intercept point (IIP3), and the operating frequency (f_c). The figure-of-merit is of the form:

$$FOM = \frac{Gain[abs] * IIP3[mW] * F_c[GHz]}{(NF-1)[abs] * P_{DC}[mW]} \quad (5)$$

where NF stands for noise figure and P_{DC} is the power dissipation and in which the gain and noise figure are expressed in their absolute values.

The summary of FOM for the three designed low-noise amplifiers together with previously published LNAs, which were the references for the LNA topology implemented in this paper, is shown in Table 4. The folded cascode LNA was presented in [7] while the shunt feedback amplifier was

TABLE IV. Comparison of the figure-of-merit for various LNAs.

Ref.	Tech. [nm]	V_{DD} [V]	f_c [GHz]	Gain [dB]	NF [dB]	IIP3 [dBm]	P_{DC} [mW]	FOM [-]
Cascoded common-source	90	1	5.8	13.796	1.7	-7.51	19.31	0.54
Folded cascode	90	1	5.8	12.893	1.79	-6.22	48.28	0.25
Shunt feedback	90	1	5.8	19.972	2.63	-5.03	56.8	0.38
[7]	90	1	5.5	15.03	2.8	-5.6	11.1	0.85
[8]	90	1.2	5	16	4	5	53	1.24

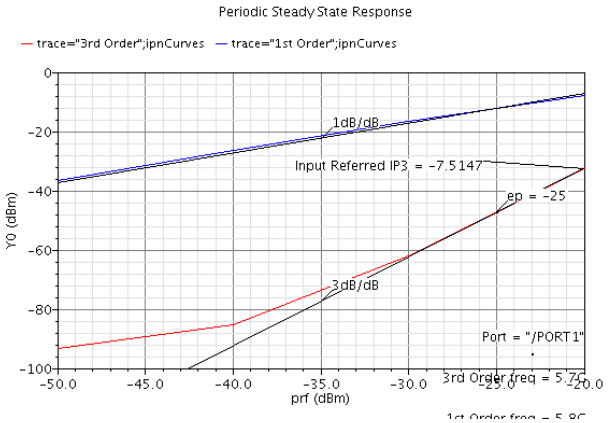

Figure 10 IIP3 of cascoded common-source amplifier.

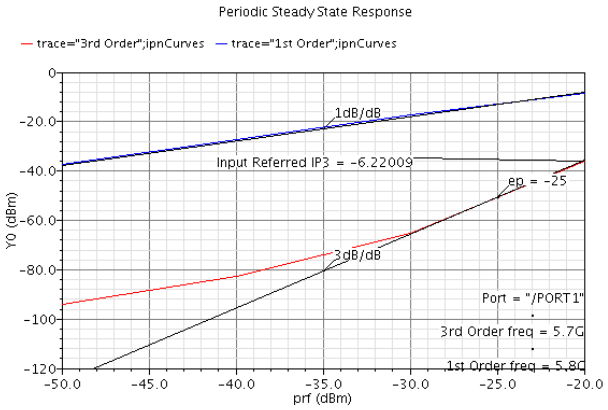

Figure 11 IIP3 of folded cascode amplifier

presented in [8]. It is seen that the cascoded common-source LNA achieved the highest FOM among the three and its FOM is comparable to previously published works. Due to the high gain and high linearity of the shunt feedback amplifier, we decided to use it in the implementation of a receiver front-end.

V. CONCLUSION

We have presented the design of three low-noise amplifiers that are viable choices in the implementation of a WiMAX receiver. The three low-noise amplifier topologies are: the cascoded common-source amplifier, the folded cascode amplifier, and the shunt feedback amplifier. The amplifiers were implemented in a standard 90-nm CMOS process

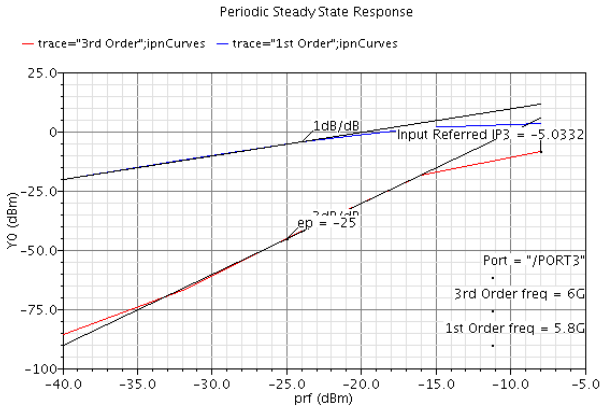

Figure 12 IIP3 of shunt feedback amplifier.

using 1-V as supply voltage. The targeted operation frequency is in the U-NII band of 5.725 GHz to 5.825 GHz.

The cascoded common-source achieved the lowest noise figure among the three due to the noise optimization in the implementation of the input matching using inductive degeneration. Since the folded cascode also shares this topology, it achieved a low noise figure comparable to the cascoded common-source. The cascoded common-source also achieved the lowest power dissipation since it contains only one current branch. The low-voltage operation capability of the folded cascode was offset by its high power consumption and further optimizations in the design are needed if it will be used in low-power applications. The shunt feedback amplifier achieved the highest gain, which is easily controlled by changing the value of the feedback resistor. The shunt feedback amplifier's highly linear performance makes it a very good choice in the implementation of a wideband receiver. Its only downside is that it has a slightly higher noise figure compared to the other two LNAs.

ACKNOWLEDGMENT

The authors would like to thank Intel Philippines, the Department of Science and Technology (DOST), the Philippine Council for Advanced Science and Technology Research and Development under DOST (DOST-PCASTRD), and the Engineering Research and Development for Technology (ERDT) for their support in this project.

REFERENCES

[1] Doan, C.H. Emami, S. Sobel, D.A. Niknejad, A.M. Brodersen, R.W. Design considerations for 60 GHz CMOS radios Communications Magazine, IEEE Volume 42, Issue 12, Dec. 2004 Page(s):132 – 140.

[2] Silicon Laboratories Introduces Industry's First Fully Integrated Single-Chip Phone For GSM/GPRS Handsets *The Free Library*. (2005, October 24). Retrieved September 22, 2009 from http://www.thefreelibrary.com/Silicon Laboratories Introduces Industry's First Fully Integrated...-a0137856788.

[3] J.Y. Lyu and Z.M. Lin. A 2-11 GHz Direct-Conversion Mixer for WiMAX Applications. TENCON 2007 - 2007 IEEE Region 10 Conference. Oct. 30 2007-Nov. 2 2007 Page(s):1 – 4.

[4] Wikipedia Contributors. WiMAX (2009, April). In Wikipedia, the free encyclopedia. Retrieved July 2009, from http://en.wikipedia.org/wiki/WiMAX.

[5] Johns, D., Martin, K., "Analog Integrated Circuit Design," Wiley, 1996.

[6] Kalantari, Fatemeh, Masoumi et al., A Low Power 90 nm LNA with an Optimized Spiral Inductor Model for WiMax Front End. Circuits and Systems, 2006. MWSCAS '06. 49th IEEE International Midwest Symposium on.

[7] Linten, D. Aspemyr, L. Jeamsaksiri, W. et al. Low-power 5 GHz LNA and VCO in 90 nm RF CMOS. VLSI Circuits, 2004. Digest of Technical Papers. 2004 Symposium on.17-19 June 2004 Page(s):372 – 375.

[8] Jacobsson, H. Aspemyr, et al. A 5-25 GHz high linearity, low-noise CMOS amplifier. Silicon Monolithic Integrated Circuits in RF Systems, 2006. Digest of Papers. 2006 Topical Meeting on.18-20 Jan. 2006 Page(s):4.

[9] IEEE standard 802.16. "Air interface for Fixed Broadband Wireless Access Systems", part 16, Oct. 1, 2004.

[10] Atallah, J. G., Rodriguez, S., Zheng, L.-R., Ismail, M. A Direct Conversion WiMAX RF Receiver Front-End in CMOS Technology. Signals, Circuits and Systems, 2007. ISSCS 2007. International Symposium on.Volume 1, 13- 14July 2007 Page(s):1 – 4. R. Brederlow et al., "A mixed signal design readmap", IEEE Design & Test of Computers, Vol.18, No.6, nov.-Dec. 2001 pp.34-36.

[11] R. Brederlow et al., "A mixed signal design readmap", IEEE Design & Test of Computers, Vol.18, No.6, nov.-Dec. 2001 pp.34-36.

[12] Lee, T., "The Design of CMOS Radio-Frequency Integrated Circuits," Cambridge: Cambridge University Press, 1998.